Synthesis of Empirical and Theoretical Approaches Toward the Establishment of GBAS σ_{pr_gnd}

Boris Pervan, Irfan Sayim, and Samer Khanafseh

(*Illinois Institute of Technology*, *Chicago*)
(Email: pervan@iit.edu)

The objective of this paper is to describe recent progress in the area of the Ground Based Augmentation System (GBAS) σ_{pr_gnd} establishment to ensure aircraft precision approach navigation integrity. In particular, this paper details: (1) the development and testing of a new adaptive binning algorithm for processing GBAS reference station empirical data to account for ranging error non-stationarity; (2) an introduction of a practical empirical method to quantify and compensate for the effects of seasonal variations of ranging error; and (3) the synthesis of these empirical results with existing theoretical ground-multipath models toward a quantitative establishment σ_{pr_gnd} for GBAS.

KEY WORDS

1. GBAS.   2. Expanding bin.   3. Sigma estimation.

1. INTRODUCTION. Applications of Global Navigation Satellite Systems (GNSS) in aviation have generated much interest in the past decade because of the potential to provide the means for aircraft navigation spanning all aspects of flight, from takeoff to touchdown, with low cost and high availability. While this has been an inspiring goal, key technical challenges exist, the most difficult of which are related to navigation integrity for precision approach and landing. The Ground-Based Augmentation System (GBAS) is the differential GNSS architecture standard for civil aircraft precision approach and landing navigation. In GBAS, navigation integrity risk is to be managed via the establishment of vertical and lateral protection levels (VPL and LPL, respectively), which define position error bounds within which navigation integrity is ensured. The prescribed algorithms for the generation of these protection levels implicitly assume zero-mean, normally distributed fault-free error distributions for the GBAS-broadcast pseudorange corrections. The broadcast corrections, in turn, are generated by averaging individual corrections obtained from multiple (typically three or four) GBAS ground receiver/antenna sets. The standard deviation of the error in the correction error for a given satellite and reference receiver is assumed by the aircraft to be equal to σ_{pr_gnd} for the satellite, which is also broadcast. Therefore, to ensure that the computed values of VPL and LPL at the aircraft are meaningful and that integrity risk is properly managed, special care must be taken by the GBAS Ground Facility (GF) in the establishment
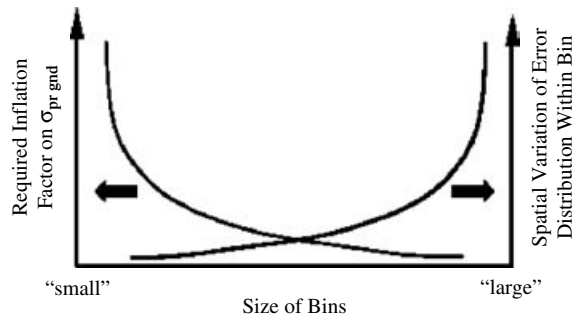
Figure 1. Effect of Bin Size on Sigma Estimation.

of the broadcast pseudorange correction error standard deviation (σ_{pr_gnd}). In this regard, the broadcast σ_{pr_gnd} must account for all contributing error sources in the ground broadcast corrections. Furthermore, the zero-mean, normal distribution with standard deviation of σ_{pr_gnd} must *overbound* the true cumulative error distribution, which in reality is not necessarily normal or zero-mean. The proper establishment of σ_{pr_gnd} is a necessary condition for GBAS integrity.

For normally distributed errors such as receiver thermal noise and diffuse multipath, standard deviations can be estimated using experimental data alone. In this case, however, it is still necessary to account for the additional integrity risk incurred by statistical uncertainty (due to finite sample size) in the knowledge of reference receiver error standard deviation and error correlation between multiple reference receivers. In related past work (Pervan and Sayim, 2001), a detailed methodology was developed to define acceptable inflation factors (from an integrity risk perspective) for the sample standard deviation as a function of the number of samples available and the sample correlation coefficient. However, in order for such an empirical process to be applied, it is first necessary to define a proper method to collect data into spatial (e.g., azimuth-elevation) bins prior to sigma estimation. While large bin sizes are desired to maximize sample size (to limit the size of the required inflation factors), bin size is ultimately constrained by the need for spatial stationarity of all data within the bin (i.e., all error data within a bin must have the same underlying distribution). The quantitative resolution of this critical trade-off, which is conceptually illustrated in Figure 1, is a major subject of the work described in this paper.

The effects of seasonal variations in pseudorange correction error, in particular multipath, must also be accounted for in the broadcast σ_{pr_gnd}. However, it is clearly impractical to collect a full-year span of data prior to commissioning for each GBAS ground facility to account for such effects. Therefore, archived error data collected at the U.S. Federal Aviation Administration (FAA) Local Area Augmentation System (LAAS) Test Prototype (LTP) facility, located at the W. J. Hughes FAA Technical Center in Atlantic City, New Jersey, is used to define a baseline GBAS ground facility model for seasonal variation in σ_{pr_gnd}. The observed LTP temporal variation can potentially be used to define a common standard inflation factor for use in the establishment of σ_{pr_gnd} in future GBAS ground facility installations until sufficient site-specific data is collected.

Because multipath error is not necessarily normally distributed, empirical data alone will not be sufficient to guarantee overbounding of the total GBAS ground

ranging error. For example, it is impossible to rely on empirically constructed distributions (e.g., error data histograms) to precisely define the actual underlying error distribution because little or no empirical data will exist in the 'tails'—which are of greatest interest for GBAS integrity. Therefore, theoretical approaches have been emphasized in past work (Brenner, et al., 1998 and Pervan, et al., 2000) to incorporate physically based ground multipath effects into σ_{pr_gnd}. Additional important research on the mathematical development of bounding non-gaussian distribution models for this purpose is described in (Braff, 2003).

The ultimate objective of prior and current research in this area is to define a sufficient methodology for the establishment of the broadcast GBAS σ_{pr_gnd} to ensure system integrity. In this paper, we describe recent progress toward this goal through: (1) the development and testing of a new adaptive binning algorithm for processing GBAS GF empirical data to account for error non-stationarity; (2) an introduction of a practical empirical method to quantify and compensate for the effects of seasonal variations of error; and (3) the synthesis of these empirical results with existing theoretical ground-multipath models toward a quantitative establishment σ_{pr_gnd} for GBAS.

2. RANGING ERROR CHARACTERISTICS. In general, the GBAS ground system ranging error has three important temporal characteristics. These are:

  I. Repeatability of multipath error from day to day (for a given satellite).
 II. Serial correlation of error over time (for a given satellite on a given day).
III. Nonstationarity of error over time (for a given satellite on a given day).

A simple illustration of data showing these characteristics is sketched in Figure 2, which shows example error (e) traces versus satellite elevation (E) for three days. In this paper, we emphasize the quantification and accommodation of these characteristics in GBAS broadcast sigma establishment rather than their causes and mitigation.

I. Repeatability (Day-to-Day Correlation): It is well known that the GBAS ground ranging error is generally repeatable (or correlated) from day to day. The repeatability characteristic is mainly caused by multipath error, and it can easily be observed with a fixed antenna when the environmental conditions are constant. Error traces typically change slowly over many days due to changes in the environment (e.g. changes in surface conditions caused by weather) and slow variations in the satellite pass geometry. The main consequence of the error repeatability effect is that sigma cannot be easily established by an ensemble of data over many days. There are two basic reasons for this: first, the data ensembled over many days will exhibit significant correlation effects between days i.e., samples are not independent; second, the sigma establishment process must be reasonably short for practical GBAS initialization. Therefore, the approach taken in this work is to generate sigma from data collected over a single commissioning day and then inflate the result to account for long-term seasonal variation of the error observed at the LTP site (where several years worth of archived data are available).

II. Serial Correlation: One of the most significant characteristics of the observed ranging error is the serial correlation between recorded samples of data.
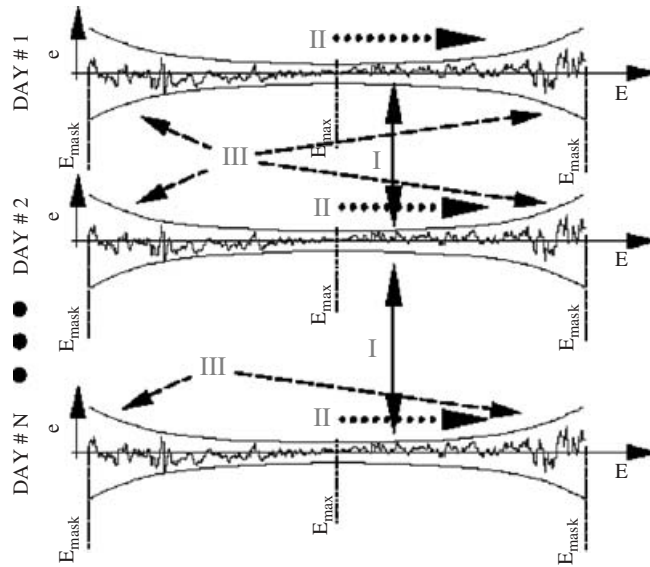
Figure 2. Basic Error Data Characteristics.

This correlation effectively limits the number of independent samples that can be assumed in the calculation of inflation factors that account for statistical uncertainty in the estimated sigma. In general, the number of independent samples for computing inflation factor will be a function of the size of the bin and the correlation time of the data within it.

III. Non-stationarity: A non-stationary process is defined as process in which statistical parameters of distribution do not stay constant in time. Elevation dependency of multipath delay and GPS antenna gain patterns are common sources of non-stationarity in observed ranging error. In GBAS, low-elevation satellites are to be tracked using a vertically stacked dipole array antenna, called the Multipath Limiting Antenna (MLA), while at high-elevation satellite tracking is done with a cross-V dipole antenna, known as the High Zenith Antenna (HZA). Together these antennas form the Integrated Multipath Limiting Antenna (IMLA) (Thornburg, et al., 2003). With the IMLA antennas the multipath contribution to non-stationarity effects are reduced, but they are nevertheless still present and can be especially significant near the cut-off angle (nominally at 35 deg elevation) between the MLA and the HZA. In addition, non-stationarity may also exist due to azimuthal error variations (caused, for example by asymmetric distribution of multipath reflectors or diffractors).

3. ADAPTIVE BINNING METHOD. The Expanding Bin (EB) method, described in this section, is a new approach for empirical sigma establishment that simultaneously manages the effects of non-stationarity and serial correlation of observed error data. Traditional approaches toward empirical sigma establishment rely on fixed bin widths, which are selected *a priori* with intent to both minimize the effect of mixing of error data derived from different distributions and maximize the number of samples within each bin. In practice, the appropriateness of prior bin size selection is difficult to quantitatively validate and is therefore often judged
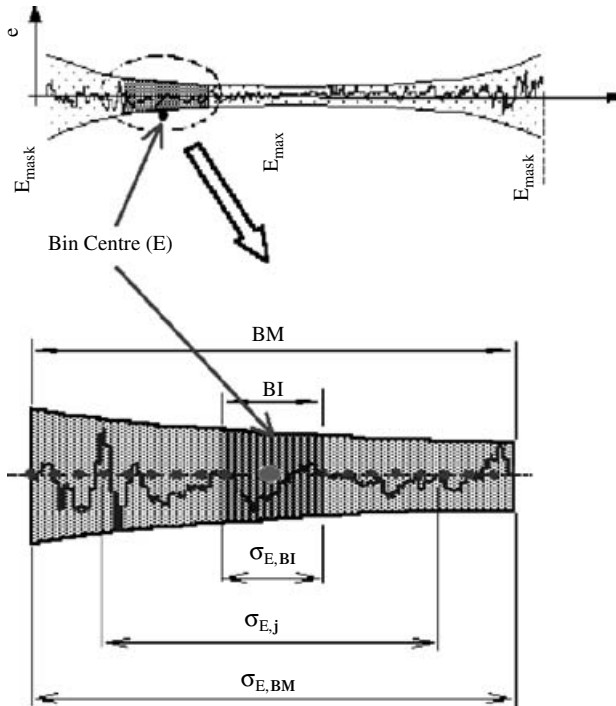
Figure 3. Fundamentals of the EB Concept.

via ad hoc inspection of the data. In contrast, the EB method is an adaptive scheme that automatically selects the bin width at a given time (or elevation) for each satellite separately. In practice, the result is achieved by considering not only a single fixed bin width but also a range of potential bin widths for the given time/elevation. The inherent trade-off in bin size selection resulting from the simultaneous presence of nonstationary and serial correlation is gracefully controlled by selecting the worst-case inflated sigma as representative of given time/elevation (E).

The EB method is implemented separately for each satellite by the following means. First, a desired bin width range is selected, with minimum and maximum bin sizes defined as *BI* and *BM*, respectively. In principle, *BM* can be selected to be the length of the entire data set and *BI* to can contain as little as two independent samples (the minimum needed to estimate standard deviation). In practice, however, a smaller range—larger *BI* and smaller *BM*—can be used because stationary will never exist over the entire data pass, and non-stationarity effects will not be present over very short time intervals (since there will be little satellite azimuth and elevation change). An illustration of example inner (core) and outer bins, *BI* and *BM* respectively, is shown in Figure 3 for an arbitrary time/elevation E. The general mathematical definition of the sigma establishment criterion for a representative sigma at time/elevation E is

$$\sigma_E = \max_{j} \sigma_{E,j} \tag{1}$$

where, j is the bin-width index ranging from *BI* to *BM*. After sigma is selected for a given time/elevation using equation (1), the entire process is repeated at next data
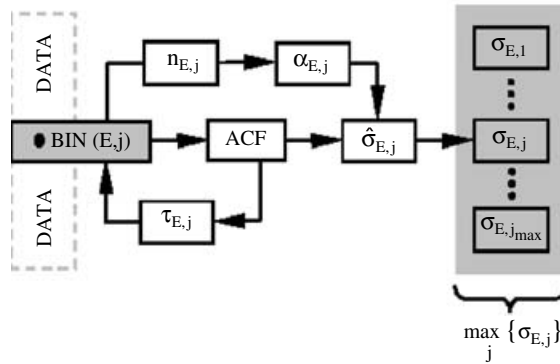
Figure 4. Flow Chart for EB Sigma Computation.

epoch until the end of the data set is reached. For a time/elevation epochs near the left- or right-hand limits of the data set, the same process is used with all available data within the BM boundary.

The actual mechanization of the actual EB process is illustrated in Figure 4. First, the sample autocorrelation function (ACF) for the selected data set is computed, and a resulting correlation time estimate is extracted from the ACF by fitting a first-order Markov model over the current bin width. Estimated correlation times smaller than the GBAS smoothing filter time constant (100 sec) are rejected and replaced by the filter time constant. In parallel, the sample variances are computed from the selected data set. The effective number of independent samples in the binned data used to generate the variance estimate is obtained by dividing the number of recorded samples in the selected data set by twice the estimated correlation time.

Based on the number of available independent samples in a given bin, an inflation factor is generated to account for statistical uncertainty in the computed sample standard deviation. The details of the computation of inflation factors from an integrity risk perspective are provided in reference (Pervan and Sayim, 2001), but for clarity in exposition here, inflation factors will be directly generated using a 99·9% confidence interval. Figure 5 shows a plot of the resulting inflation factor as a function of the number of independent samples. It is clear that as the number of independent samples becomes smaller the inflation factor on sigma to cover estimation uncertainty will increase. For each candidate bin size, the computed sample standard deviation is inflated and the result is stored. When all candidate bin sizes are processed, the upper bound inflated sigma is selected:

$$\sigma_{m,E}^{s} = \max_{j} \sigma_{m,E,j} = \max_{j} \alpha(n_{m,E,j})\hat{\sigma}_{m,E,j} \tag{2}$$

where $\alpha(n_{m,E,j})$ is the inflation factor given that $n_{m,E,j}$ independent samples are available for reference receiver m, time epoch E, and bin width index j. $\hat{\sigma}_{m,E,j}$ is the computed sample standard deviation for receiver m, time epoch E and bin width index j.

Figure 6 shows an example ranging error history obtained at the LTP for a typical satellite pass. The thick black trace shows the sigma profile generated using the EB method. The sigma vs. time profile is a faithful representation of the variation of
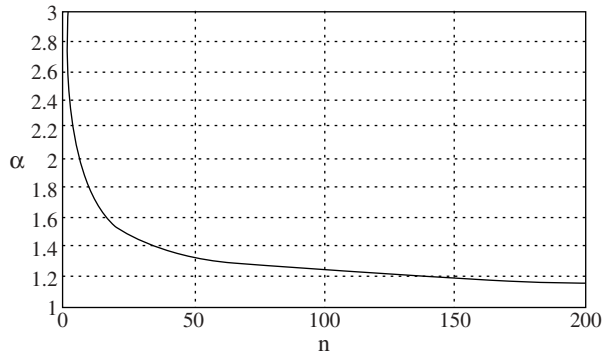
Figure 5. Inflation for Statistical Uncertainty in Sigma Estimation as a Function of Independent Sample Size (99·9% Confidence).
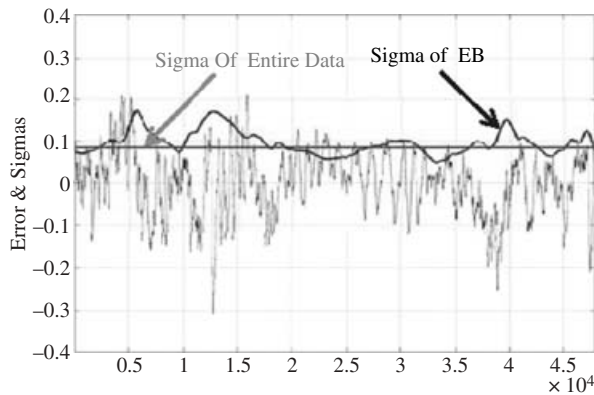

Figure 6. Sigma Generation for Nonstationary Process.

the error data itself, because it is influenced both by the slow variation of error (serial correlation effect) and the time-varying magnitude (non-stationarity) of the error data. In contrast, the grey horizontal line in the figure shows the inflated sigma obtained using the entire data set (without regard to non-stationarity effects); it is obvious that the sigma computed this way cannot capture error variations in time.

A comparison of the two sigma-estimation approaches is shown in the cumulative distribution function (CDF) plots in Figure 7. In this figure, the performance of both methods is compared against a standard normal distribution by normalizing the actual error data by each of the two computed sigma curves and then plotting the corresponding CDFs. It is clear from the figure that for the EB-normalized case, the standard normal distribution overbounds the EB-normalized error data with a significant margin. In contrast, the standard normal distribution does not overbound the error data normalized by the inflated sigma of the entire data set. The reason for this is that the latter approach does not account for nonstationarity (i.e., mixing of data from different error distributions during the satellite pass).
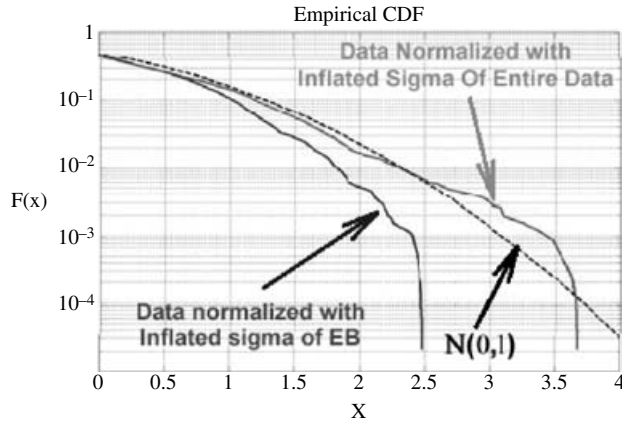
Figure 7. Cumulative Distribution Performance.

4. CORRELATION BETWEEN REFERENCE RECEIVERS. In the GBAS V/LPL computations, it is implicitly assumed that ranging errors are uncorrelated across ground receivers. In fact, the existence of any such correlation is not strictly consistent with the standardized V/LPL equations since $\sigma^2_{pr\_gnd}$ for an individual reference receiver is always divided by the number of receivers to account for the averaging of uncorrelated receiver measurements (RTCA, 1998). In reality, however, it is possible (even likely) that some measurable correlation between receivers will exist. Furthermore, even if a negligibly small correlation coefficient is computed from a finite sample set, the statistical uncertainty in the estimate must also be accounted for. Such uncertainty is lessened, as one would naturally expect, as the sample size used to estimate correlation coefficient increases.

To accommodate the effects of correlation, we begin with the ground error standard deviation for any given reference receiver as expressed by equation (2). The effect of measured error correlation between receivers (when averaging over M reference receivers) can be modelled as an increase in broadcast sigma as follows:

$$\sigma^{sc}_{m,E} = \beta_m \sigma^s_{m,E} \tag{3}$$

where

$$\beta_m = \begin{cases} \sqrt{1 + \displaystyle\sum_{\substack{i=1 \\ i \neq m}}^{M} \rho_{mi}} & \displaystyle\sum_{\substack{i=1 \\ i \neq m}}^{M} \rho_{mi} \geq 0 \\[4ex] 1 & \displaystyle\sum_{\substack{i=1 \\ i \neq m}}^{M} \rho_{mi} < 0 \end{cases} \tag{4}$$

where ρ_{mi} is the correlation coefficient for receivers m and i. Note that any inflation of sigma due to negative correlation is irrelevant since the initial (implicit) assumption of uncorrelated receiver errors will already result in over-inflation in this case.
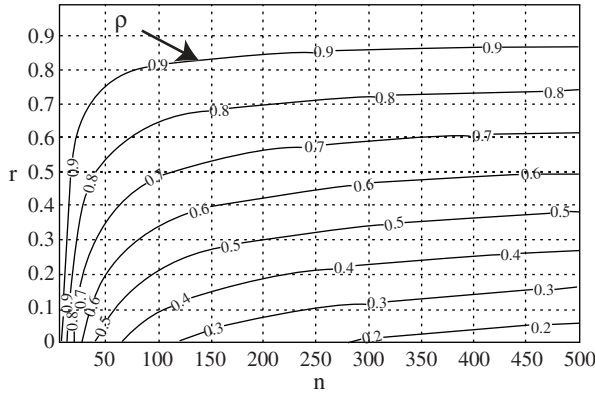
Figure 8. Contours of 99·9% Confidence Correlation as a Function of Measured Correlation and Independent Samples.

The correlation coefficients used in equation (4) must be computed from the empirical error data for individual receivers. The statistical relationship between a computed correlation coefficient r, generated using n samples of empirical data, and the actual underlying correlation coefficient correlation ρ is defined in (Bendat and Piersol, 1986) as

$$\frac{1}{2} \ln\left(\frac{1+r}{1-r}\right) \sim N\left[\frac{1}{2}\ln\left(\frac{1+\rho}{1-\rho}\right), \frac{1}{\sqrt{n-3}}\right], \tag{5}$$

where N represents the normal distribution function whose first and second arguments are its mean and standard deviation, respectively. A detailed methodology for the selection of correlation coefficient ρ (given r and n) to ensure overall integrity risk requirements is described in reference (Pervan and Sayim, 2001). Again, however, for the sake of clarity and simplicity in this exposition, it is sufficient to use the 99·9% upper confidence values for ρ. These are plotted as contours in Figure 8 versus r and n.

5. SEASONAL VARIATION OF RANGING ERROR.   In this section, a practical procedure for quantification and accommodation of temporal variation of errors is described. The process is based on the observed relative maximum variation between average sigmas across seasons. The goal is to establish sigma from a limited duration of LGF commissioning data (as short as one day), using the correlation-adjusted EB estimate σ_E^{sc}, and scale by a factor (γ_m), derived from long-term archived LTP data, to account for temporal variation:

$$\sigma_{m,E}^{sct} = \gamma_m \sigma_E^{sc} \tag{6}$$

The long-term temporal variation factor (γ_m) is obtained using a one-year span of LTP data, with four seasonal samplings of two weeks per season. Each day of archived LTP data consists of error measurements from three LAAS Integrated

Multipath Limiting Antennas (IMLAs). Using the initial day's worth of data for a given satellite, a sigma profile can be established using the EB algorithm. All of the ranging errors on the subsequent days of data for this satellite are normalized by the initial day's EB sigma values. This is done so that the effects of temporal variation relative to the initial day's EB result can be directly observed. Next, the standard deviations of each normalized error data set are computed and grouped into four averaged seasonal samplings. The reason for seasonal grouping and averaging of sigmas is that we are interested here in characterizing the effects of long-term, slowly varying effects due to the weather-related environmental changes. Finally, the average standard deviation of each season is sorted from minimum to maximum, and the ratio between maximum and minimum average sigma is defined as the temporal variation scale factor (γ_m) as shown:

$$\gamma_m = \max(\sigma_{m,seasons})/\min(\sigma_{m,seasons}) \qquad (7)$$

where $\sigma_{m,seasons} = [\bar{\sigma}_{m,winter} \ \ \bar{\sigma}_{m,spring} \ \ \bar{\sigma}_{m,summer} \ \ \bar{\sigma}_{m,fall}]$, and $\bar{\sigma}_{m,winter}$, $\bar{\sigma}_{m,spring}$, $\bar{\sigma}_{m,summer}$, and $\bar{\sigma}_{m,fall}$ are averages of normalized error standard deviation for the winter, spring, fall, and summer seasons, respectively. When for example this process is applied to archived LTP (year 2000) data for reference receiver (RR) 1 for an example satellite, GPS PRN 2, the seasonal variation inflation factor result is $\gamma_1 = 1\cdot14$. A comprehensive, but otherwise identical, analysis for multiple satellites and receivers must be conducted to define a generalized seasonal variation inflation factor suitable for use in the GBAS ground sigma establishment process.

6. GROUND REFLECTION MULTIPATH. Due to the slowly varying nature of ground-reflection multipath, it is unlikely that sigma can be established by experimental means alone. Therefore, in past work, a number of candidate theoretical approaches were defined to statistically model ground multipath effects. A relatively conservative model, using a uniformly distributed relative phase and constant (maximum) strength of the reflected multipath signal, is selected here as a representative example. For this model, it is shown (Pervan, et al., 2000) that ground reflection multipath can be bounded by a zero mean Gaussian distribution with standard deviation

$$\sigma_{MP,E} \geq 1\cdot05(D/U)\min[2h\sin E, d], \qquad (8)$$

where D/U is the amplitude of reflected signal relative to direct, h is antenna height, E is elevation angle, d is the half correlator spacing in meters (e.g., $0\cdot05$ chip $= 15$m is used in this work). In Figure 9, $\sigma_{MP,E}$ is shown in the lower plot using the values of relative signal strength D/U given in the upper plot, which were obtained from (Braff, 1997).

While the ground reflection multipath resulting from the selected model is not Gaussian, it is shown (Pervan et al., 2000) that if the bounding value of multipath sigma in equation (8) is combined via root-sum-square with sigmas from other Gaussian error sources, Gaussian overbounding is preserved. This is an important result that is relevant to the sigma synthesis discussion given in the next section.
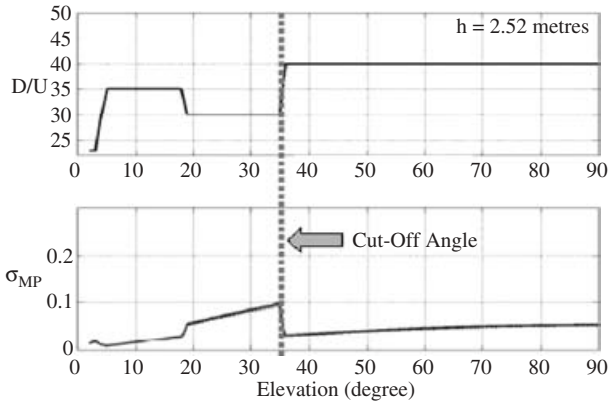
Figure 9. Ground Multipath Sigma vs. Satellite Elevation Angle.

7. SYNTHESIS OF BROADCAST SIGMA. To accommodate all contributing elements, establishment of broadcast sigma must include:

I- Sigma estimated from empirical data ($\sigma_{M,E}^{comp}$). The EB adaptive bin method is used here to account for the time correlation and non-stationarity (mixing) of error data within bins,

- A limited (one day) data analysis for every new installation and sigma must include:
  - Inflation due to sample standard deviation uncertainties (α).
  - Inflation due to correlation between receivers (β).
- Seasonal Data Analysis of archived LTP data provides:
  - Inflation due to long-term temporal variation (γ).

II- Sigma generated from theoretical bounds and analysis ($\sigma_{MP,E}$). To accommodate ground reflection multipath error sources, a theoretical model must be defined. The example model used here is the ground reflection multipath model from reference (Pervan, et al., 2000).

III- Sigma generated from receiver noise model ($\sigma_{RN,E}$). Ranging error standard deviations due to ground receiver noise and interference are a function of the measured signal-to-noise ratio and must also be accounted for in the broadcast σ_{pr_gnd}. Existing models for this effect may be found in (McGraw, et al., 2000) and (Enge, 1999).

The sigma establishment process can now be defined as follows:

1. Use the EB method to generate the maximum obtainable sigma values from data. The EB approach implicitly incorporates non-stationarity effects and inflation for sample standard deviation for estimation uncertainty.

$$\sigma_{m,E}^{s} = \max_{j} \left\{ \sigma_{m,E,j} \right\} = \max_{j} \left\{ \alpha_{m,E}(n_{m,E,j}) \hat{\sigma}_{m,E,j} \right\} \qquad (9)$$

2. Account for correlation effects between reference receivers.

$$\sigma_{m,E}^{sc} = \beta_{m} \sigma_{m,E}^{s} \qquad (10)$$

3. Account for long-term temporal (seasonal) error variation.

$$\sigma_{m,E}^{sct} = \gamma_m \sigma_E^{sc} \tag{11}$$

4. Generate the composite sigma from data.

$$\sigma_{pr\_gnd,E}^{\mathrm{I}} = \sigma_{M,E}^{comp} = \sqrt{\frac{\sum_{m=1}^{M} \left(\sigma_{m,E}^{sct}\right)^2}{M}} \tag{12}$$

5. Combine composite sigma with the theoretical multipath sigma bound,

$$\sigma_{pr\_gnd}^{\mathrm{II}} = \sqrt{\left(\sigma_{pr\_gnd,E}^{\mathrm{I}}\right)^2 + \sigma_{MP,E}^2} \tag{13}$$

6. Combine composite sigma and receiver noise standard deviation to generate the final value broadcast value.

$$\sigma_{pr\_gnd} = \sqrt{\left(\sigma_{pr\_gnd,E}^{\mathrm{II}}\right)^2 + \sigma_{RN,E}^2} \tag{14}$$

The standard deviation of ranging error obtained in equation (12) is a purely empirical result and forms the basis estimate for the broadcast sigma. In the next step, the composite sigma obtained using equation (13) is a conservative representation of broadcast correction error standard deviation since it explicitly accounts for ground reflection multipath error theoretically, even though some of ground reflection multipath may already be captured empirically in equation (12). The last model, equation (14), is an even more conservative result because receiver noise may also be captured by both theoretical and empirical means. Since $\sigma_{RN,E}$ is typically very small (less than 3 cm for the IMLA) it will not be considered further in this paper. For the interested reader, additional details on receiver noise are provided in (McGraw, et al., 2000) and (Enge, 1999).

8. AN ILLUSTRATIVE EXAMPLE RESULT. In the following example, the procedure just described was executed using archived LTP data to obtain a broadcast sigma based on equation (13). The data and processing specifications used for this example are listed below:

- Site: FAATC/LAAS Test Prototype
- *Time of Data Record:* February 2000
- *Number of Reference Receivers:* 3
- *Raw Data Sample Rate:* 2 Hz
- *Satellite:* PRN#2
- *Elevation Mask:* 5 degree
- *Cut-Off Angle between MLA and HZA:* 35 deg
- *C/NO Mask:* 40 dB-Hz
- *Smoothing Time Constant:* 100 sec.
- *BI:* 1000 Recorded Samples
- *BM:* 5000 Recorded Samples
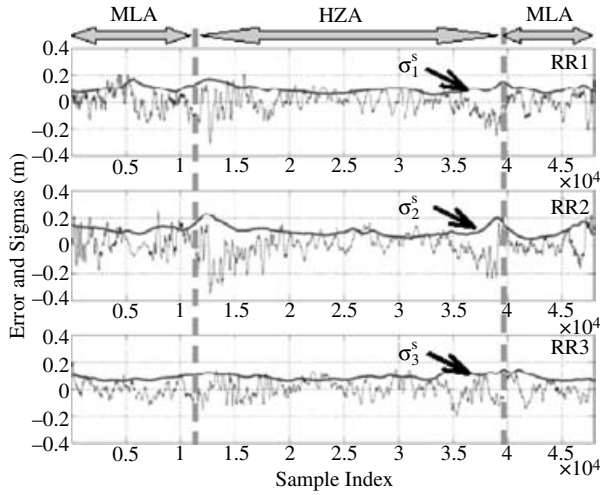- *Conf. Interval for Inflation:* 99·9%

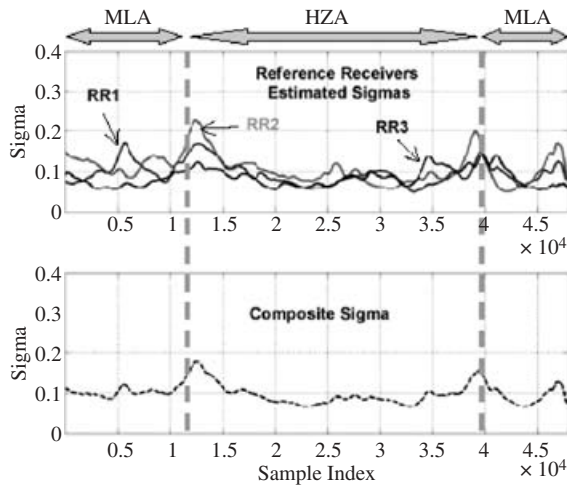Figure 10. EB-Generated Sigma for Each RR.

Figure 11. Sigma Traces for Individual RRs and Composite (Average Across RRs).

Following the prescribed process, sigmas are first estimated by direct use of data with the EB method. Each sigma trace is then plotted (solid curve) in Figure 10 for each of the three reference receivers (RRs). For comparison with the computed sigma traces, the actual error data is also plotted. It is observed that the worst sigma values are obtained near transition (cut-off) elevation angles (vertical dashed lines) between HZA and MLA. For more direct comparison of relative performance between reference receivers the sigma traces of Figure 10 are reproduced in the upper plot of Figure 11. The lower plot in the same figure shows the composite (average) sigma of three RRs ($\sigma_{M,E}^s$). The composite broadcast sigma of three-reference receivers is about 10 cm except near transition (cut-off) angle regions. The EB-sigma-normalized error distributions (CDFs) for the three receivers are plotted in Figure 12. It is clear

Table 1. Correlation Values.

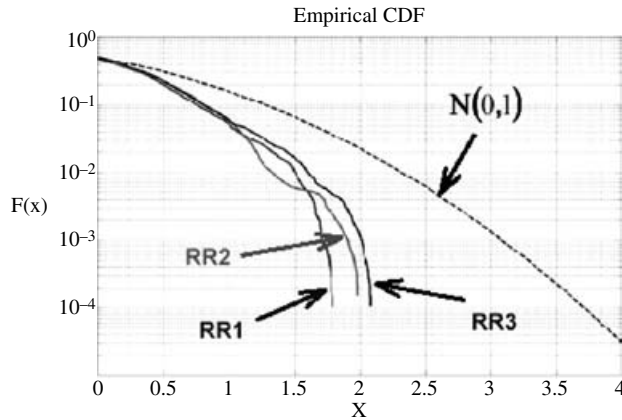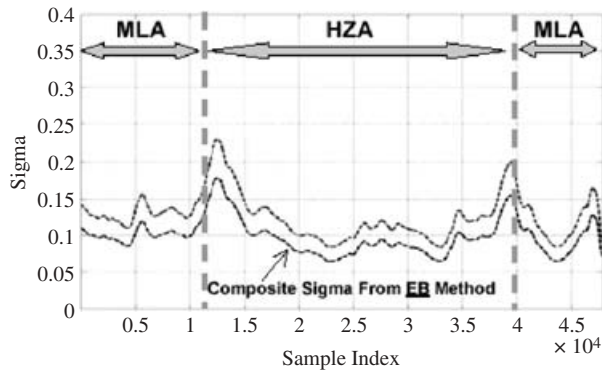| r/ρ	m = 1	m = 2	m = 3	β
m = 1	1	0·21/0·38	0·19/0·37	1·3264
m = 2	0·21/0·38	1	0·03/0·22	1·2711
m = 3	0·19/0·37	0·03/0·22	1	1·2638

Figure 12. CDF Overbound Using EB-Generated Sigmas.

Figure 13. Composite Sigma Traces Before and After Inflation for RR Correlation.

that each reference receiver's normalized error is conservatively overbounded by a standard normal CDF.

Correlation effects between receivers are accounted for next. In Table 1, the measured (r) and confidence-inflated (ρ) values of correlation between reference receivers are given. The correlation sigma inflation factors (β), computed using equation (4), are listed in the last column of the table. Figure 13 shows the resultant composite sigma trace (upper curve) when the correlation effects are accounted for using equation (10).
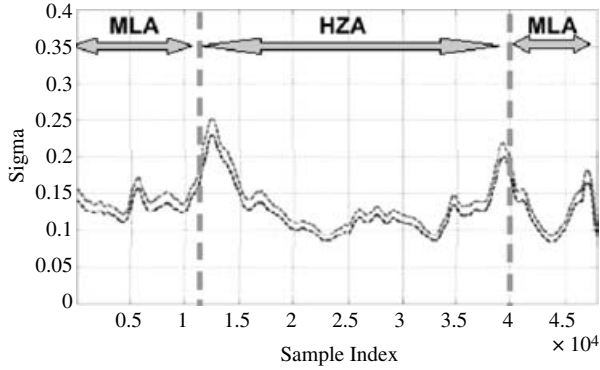
Figure 14. Composite Sigma Traces Before and After Inflation for Temporal Variation.
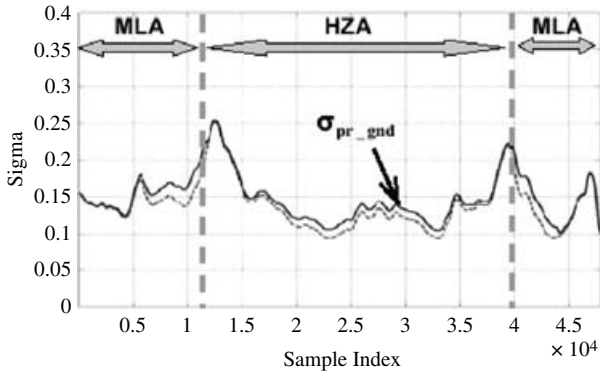

Figure 15. Composite Sigma Traces Before and After Adjustment for Ground Multipath Effects.

In Figure 14, the effect of temporal variation is applied to sigma after correlation effects have been applied (composite $\sigma_{m,E}^{sct}$). For the purposes of this quantitative example, we assume that the temporal inflation factors for the three receivers are the same (i.e., $\gamma_1 = \gamma_2 = \gamma_3 = 1\cdot14$). The upper curve in Figure 14 is then the final sigma trace ($\sigma_{pr\_gnd}^{I}$) obtained from direct analysis of all the available empirical data.

In Figure 15, the theoretical ground reflection multipath sigma ($\sigma_{MP,E}$) from equation (8) and Figure 9 is combined with the empirically obtained result of Figure 14 to get $\sigma_{pr\_gnd}^{II}$. The final composite broadcast sigma result, σ_{pr_gnd}, is plotted in Figure 16, where it is compared with current LGF C3 and B3 broadcast sigma specifications (RTCA, 1998). It is evident from the figure that, for this example, the established σ_{pr_gnd} is greater than the C3 and B3 specifications and therefore must be reduced to ensure compliance. Fortunately, there are several methods that can be effective in this regard:

1. The MLA antenna exhibits code-minus-carrier variations (as a function of elevation angle) that result in repeatable, systematic errors in the raw empirical data that can exceed 10 cm. For the raw data used in this example, a coarse calibration (based on earlier archived empirical data) was performed to
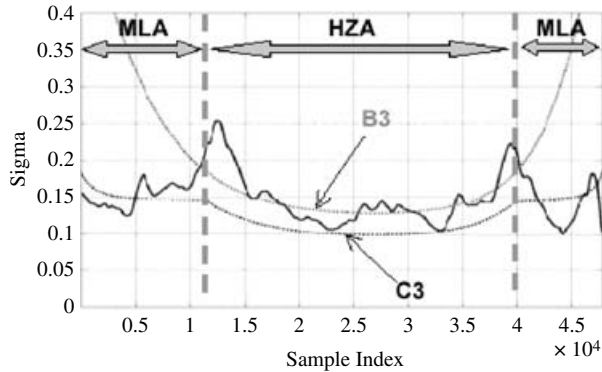
Figure 16. Final Sigma Result vs. Specifications.

partially account for this effect. However, a more careful antenna calibration will clearly be required prior to system commissioning. The result is that much cleaner raw data sets will be input into the EB algorithm, which in turn, will produce smaller sigmas.

2. The transition angle (cut-off angle) between HZA and MLA can be varied to some extent (about ± 5 deg) to minimize the sigma peaks.

3. For certain elevations, the sigma performance of one or two receivers may be acceptable without the aid of the remaining receiver(s), which may have higher sigmas. For this example, RR 3 has lower error than the other two receivers near the peaks at 35 deg. Therefore, individual RR masking at certain elevations where sigma is large may prevent unacceptable composite sigma results.

9. CONCLUSIONS. In this paper, a new adaptive bin selection approach for GBAS/LAAS sigma estimation, known as the Expanding Bin (EB) method was developed and successfully applied to non-stationary and autocorrelated ranging error data for establishment of LGF broadcast sigma. The results in this paper show that:

● Using the EB method, the upper-bound sigma trace (as a function of time/ elevation during the satellite pass) is directly extracted from the available data.
● The EB-method implicitly accounts for non-stationarity and inflation for statistical uncertainty simultaneously.
● Error data normalized by EB-sigmas are conservatively overbounded by a standard normal CDF.
● Abrupt variations in sigma across bin boundaries, which exist in the fixed-bin approaches, are naturally eliminated using the EB approach.

An analysis of long-term (seasonal) error variation was performed for a single prototype reference receiver/antenna. The maximum normalized sigma variation observed in seasonally sampled archived LTP data was used to define the relevant inflation factor to account for temporal variation. The methodology was recommended for use of newly commissioned LGF sites until sufficient site-specific data is collected. In addition, the effects of correlation between receivers and prior

theoretical results for non-Gaussian ground reflection multipath errors were directly addressed and accounted for in this paper.

Finally, a complete methodology was presented to incorporate all of these contributing error sources in the final establishment of broadcast sigma. The methodology is based on a synthesis of empirical and theoretical results.

ACKNOWLEDGEMENTS

REFERENCES

Bendat, J. S. and Piersol, A. G. (1986), *Random Data Analysis and Measurement Procedures*, 2nd Edition, John Wiley & Sons.

Braff, R. (1997), Description of the FAA's Local Area Augmentation System (LAAS), *NAVIGATION: Journal of the Institute of Navigation*, **44**, No. 4.

Braff, R. (2003), A Method of Fault-Free Overbounding Using a Position Domain Monitor, *Proceedings of The Institute of Navigation National Technical Meeting*, Anaheim, California.

Brenner, M., Reuter, R., and Schipper, B. (1998), GPS Landing System Multipath Evaluation Techniques and Results, *Proceedings of the 11th International Meeting of the Satellite Division of the Institute of Navigation* (*ION GPS-1998*), Nashville, TN.

Enge, P. (1999), Local Area Augmentation of GPS for the Precision Approach of Aircraft, *Proceedings of the IEEE*, **87**, 111–132.

McGraw, G. A., Brenner, M., Pullen, S. and Van Dierendonck, A. J. (2000), Development of the LAAS Accuracy Models," *Proceedings of the 13th International Meeting of the Satellite Division of the Institute of Navigation* (*ION GPS-2000*), Salt Lake City, UT.

Pervan, B., Pullen, S., and Sayim, I. (2000), Sigma Estimation, Inflation and Monitoring in the LAAS Ground System, *Proceedings of the 13th International Meeting of the Satellite Division of the Institute of Navigation* (*ION GPS-2000*), Salt Lake City, UT.

Pervan, B and Sayim, I. (2001), Sigma Inflation for the Local Area Augmentation of GPS, *IEEE Transactions on Aerospace and Electronic Systems*, **37**, 1301–1310.

RTCA, Inc. (1998), Minimum Aviation System Performance Standards for the Local Area Augmentation System (LAAS), RTCA/DO-245.

Thornburg, D. B., Thornburg, D. S, DiBenedetto, M. F., Braasch, M. S., van Graas, F. and Bartone, C. (2003), LAAS Integrated Multipath Limiting Antenna, *NAVIGATION: Journal of the Institute of Navigation*, **50**, No. 2.